



A dynamic local scale vegetation model for lycophytes (LYCOM)

Suman Halder¹, Susanne K. M. Arens², Kai Jensen^{3,*}, Tais Wittchen Dahl^{4,*}, and Philipp Porada⁵

¹Universität Hamburg, Institut für Pflanzenwissenschaften und Mikrobiologie, Ohnhorststraße 18 22609 Hamburg, Tel.: +49 40 42816-579

²University of Copenhagen, Øster Voldgade 5-7, 1350 København K, Tel.: +45 35 33 09 27

³Universität Hamburg, Institut für Pflanzenwissenschaften und Mikrobiologie Angewandte Pflanzenökologie Ohnhorststr. 18 22609 Hamburg, Tel.: +49 40 42816-576

⁴University of Copenhagen, Øster Voldgade 5-7, 1350 København K, Tel.: +45 35 32 23 56

⁵Universität Hamburg, Institut für Pflanzenwissenschaften und Mikrobiologie Angewandte Pflanzenökologie Ohnhorststraße 18 22609 Hamburg, Tel.: +49 40 42816-577

Correspondence: Suman Halder (suman.halder@uni-hamburg.de)

Abstract. Lycophytes (club mosses) represent a distinct lineage of vascular plants with a long evolutionary history including numerous extant and extinct species which started out as herbaceous plants and later evolved into woody plants. They enriched the soil carbon pool through newly developed root-like structures and promoted soil microbial activity by providing organic matter. These plants enhanced soil carbon dioxide (CO₂) via root respiration and also modified soil hydrology. These effects had the potential to promote the dissolution of silicate minerals, thus intensifying silicate weathering. The weathering of silicate rocks is considered one of the most significant geochemical regulators of atmospheric CO₂ on a long (hundreds of thousands to millions of years) timescale. The motivation for this study is to achieve an increased understanding of the realized impacts of vascular plants, represented by modern relatives to the most basal plants with vascular tissue and shallow root system, on silicate weathering and past climate. To this end, it is necessary to quantify physiological characteristics, spatial distribution, carbon balance, and the hydrological impacts of early lycophytes. These properties, however, cannot be easily derived from proxies such as fossil records, for instance. Hence, as a first step, a process-based model is developed here to estimate net carbon uptake by these organisms at the local scale, considering key features such as biomass distribution above and below ground, root distribution in soil regulating water uptake by plants besides, stomatal regulation of water loss and photosynthesis, and not withholding respiration in roots. The model features ranges of key physiological traits of lycophytes to predict the emerging characteristics of the lycophyte community under any given climate by implicitly simulating the process of selection. In this way, also extinct plant communities can be represented. In addition to physiological properties, the model also simulates weathering rates using a simple limit-based approach and estimates the biotic enhancement of weathering by lycophytes. We run the Lycophyte model, called LYCOM, at seven sites encompassing various climate zones under today's climatic conditions. LYCOM is able to simulate realistic properties of lycophyte communities at the respective locations and estimates values of Net Primary Production (NPP) ranging from 126 g carbon m⁻² year⁻¹ to 245 g carbon m⁻² year⁻¹. Our limit-based weathering model predicts a mean chemical weathering rate ranging from 5.3 to 45.1 cm ka⁻¹ rock with lycophytes varying between different sites, as opposed to 0.6 - 8.3 cm rock ka⁻¹ without lycophytes, thereby highlighting the potential importance of such vegetation at the local scale for enhancing chemical weathering. Our modeling study establishes a basis for



25 assessing biotic enhancement of weathering by lycophytes at the global scale and also for the geological past. Although our method is associated with limitations and uncertainties, it represents a novel, complementary approach towards estimating the impacts of lycophytes on biogeochemistry and climate.

1 Introduction

30 The increasing carbon dioxide (CO₂) content of the atmosphere is one of the most discussed topics in climate research pertaining to the rising concerns over the aggravating impacts of its greenhouse effect. Since societal well-being closely connects to the level of CO₂ in the atmosphere, it is important to look at the past developments and understand the key events which ensued changes in the level of CO₂ in the atmosphere. Foster et al. (2017) showed the fluctuation of CO₂ content of the Earth's atmosphere through the history of Earth and there have been several attempts to explain the rapid depletion around 420 million years ago. It was around the same time when the advent of the earliest lycophytes was recorded from the study of fossils (Matsunaga and Tomescu, 2016; Thomas and Watson, 1976).

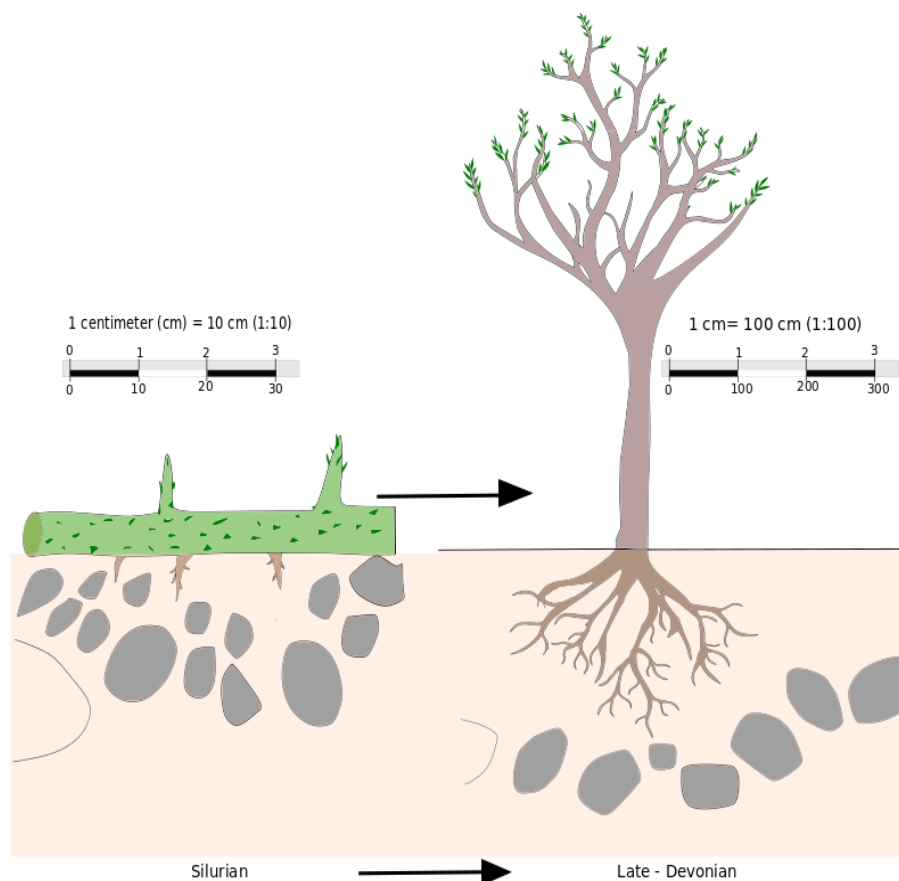
35 Lycophytes or club mosses are regarded as the earliest forms of extant vascular plants (tracheophytes) with a long evolutionary history (Dahl and Arens, 2020). This ancient group of vascular plants (Qiu et al., 2006; Wickett et al., 2014) dates back to the Mid Ordovician (Rubinstein et al., 2010; Steemans et al., 2009), and later evolved tree stature in the Mid-Devonian (Stein et al., 2012) before surpassing a height of 50 meters during the Carboniferous period (Gensel and Berry, 2001; Taylor et al., 2009). This long transformative history along with a rich fossil record and extant diversity have made studies of lycophytes 40 central to plant evolution. In any case, Lycophytes were not only abundant during the Carboniferous period but became ecologically significant much earlier in the late Silurian (Wellman et al., 2013) and soon dominated the flora. The dominant role of lycophytes as terrestrial vegetation in those periods could be attributed to the appearance of root-like structures (Matsunaga and Tomescu, 2016) coupled with stomatal control (Brodribb and McAdam, 2011) for controlling water loss.

45 Root evolution has been a gradual process and Fig. 1 depicts the transformation from its early elementary stages of appearance in lycophytes to a sophisticated structure comparable to the roots of modern plants during the Devonian. It is without a doubt that the transformation took place over a considerable period. In fact, this evolution led to the foundation of modern plants and trees which are characterized by complex tissue structure allowing transport of water and nutrients, thus making high rates of Net Primary Production (NPP) possible. Root-like structures have been observed in fossil records dating back to as early as 413 million years (Hao et al., 2010) in the early Devonian (Gensel et al., 2001). This innovation might have 50 been central to the dominance of flora on the planet and enabled plants to grow in size as well as overcome the physiological drawback of their dependence on moist habitats (Bateman et al., 1998).

55 Roots provided the lycophytes with a key interface for interaction with the terrestrial environment for their nutrient and water supply as they could utilize the underground reserves which remained untouched before. Roots provided an anchorage, which may have been a precondition for the development of the first trees. This effect also increased soil stability, hence it potentially reduced the erosion rate (Vannoppen et al., 2017). Roots influenced hydrological processes such as water uptake and enhanced water loss through plants according to the atmospheric and physiological demand, thereby altering the water cycle. The other



Figure 1. A conceptual diagram of evolution of roots from its earliest stage in the Silurian era to a sophisticated form during the Devonian



notable consequence of root development is believed to be an enhancement of chemical weathering, which could have had strong impacts on atmospheric CO₂ content and the Global carbon budget.

In general, the weathering regime is often influenced by several factors, and plants, and their associated microorganisms have been suggested to have a substantial impact on weathering, through respiration in the soil, hence increasing the partial pressure of soil CO₂ to several-fold greater than the atmospheric CO₂ level (Kelly et al., 1998; Montanez, 2013). In addition to plant-derived organic matter respired by these microorganisms, the root respiration also adds to the soil CO₂ content, thus increasing soil acidity and influencing weathering rates (Moulton et al., 2000; Andrews and Schlesinger, 2001; Berner et al., 2003).

Roots were not the only suite of innovations from these kinds of plants, they further developed stomatal control of water loss to be able to photosynthesize under adverse climatic conditions which might have given lycophytes yet another advantage over their contemporaries. The evolution of stomata followed the innovation of roots closely, around 400 million years before the present. Water loss and NPP are regulated by the opening and closing of stomata. By changing the aperture of the



70 stomata, plants inhibit water loss to prevent desiccation, at the cost of reduced photosynthetic productivity. The combination
of adjustable stomata with an internal water transport system i.e. vascularity, was a turning point in plant evolution that might
have enabled vascular plants to invade most terrestrial environments, tolerating water stress and exploiting favorable conditions
(Raven, 2002). The development of such traits in lycophytes was gradual and was initially, relatively primitive. Brodribb and
McAdam (2011) suggested that lycophyte and fern stomata lacked key responses to abscisic acid and epidermal cell turgor,
making stomatal behavior highly predictable. The stomatal regulation of water loss was determined solely by the surrounding
75 environmental conditions due to a poorly developed hydraulic system (Boyce and Lee, 2010), unlike today's plants which have
a more complex mechanism driving the stomatal control.

The stomatal development primarily impacted and regulated water loss through transpiration, which may have had a signif-
icant role in altering the global water cycle, in particular by increasing the land surface area affected by precipitation through
the recycling of water vapor (Berner, 1992; Drever, 1994; Ibarra et al., 2019). This may have then indirectly contributed to the
80 alteration of weathering rates via an enhancement of local and global water recycling as well as increasing the area available for
weathering in the interiors of continents (Shukla and Mintz, 1982; Boyce and Lee, 2010, 2017). The moisture recycling likely
also increased plant productivity, thus increasing soil CO₂ content across continents. Consequently, the presence of land plants
increased the quantity of water in continental interiors available for weathering and increased primary productivity, further
contributing to an increase in global weathering.

85 Silicate weathering is considered as one of the most significant geochemical regulators of atmospheric CO₂ on a long (hun-
dreds of thousands to millions of years) timescale (Berner, 1990). Silicate weathering is primarily mediated by the hydrological
cycle (Walker et al., 1981; Bluth and Kump, 1994; Maher, 2011; Maher and Chamberlain, 2014; Green et al., 2017; Ibarra et al.,
2019) and it serves as a dominant carbon sink for Earth in the long run (Berner, 1998; Bergman et al., 2004; Gibling et al.,
2014). A precondition for the weathering reactions is the production of weak carbonic acid from rainwater and soil CO₂, which
90 dissociates into bicarbonate (HCO₃⁻) ions during the dissolution of silicate minerals. The ions subsequently enter streams via
runoff and eventually the oceans where they are used by various organisms to build shells and skeletons. These then serve as
a long-term carbon sink after sedimentation. Hence the weathering of silicate rocks corresponds closely to the flux of carbon
from the atmosphere into seafloor sediments.

This so-called silicate weathering feedback might have been significantly influenced over various periods of Earth's history
95 following the further evolution of plants and the development of roots and stomata. The increased soil carbon pool had the
potential to promote the dissolution of silicate minerals (Walker et al., 1981). The study by Matsunaga and Tomescu (2016)
demonstrates a substantial plant–substrate interaction that was already underway in the Devonian, causing weathering by root
penetration, and thereby confirming the significance of such an advent of vascular vegetation. Further studies have already
claimed an enhancement of chemical weathering by vascular plants to have exceeded six-folds as compared to their earlier
100 counterpart, i.e. non-vascular vegetation (Cochran and Berner, 1993), along with an improved pedogenesis (Quirk et al., 2015).

Although lycophytes were abundant in the Silurian, their effects on weathering rates remain unclear. Detailed information
on physiology, productivity, spatial distribution, and hydrological properties of these early plants, which is crucial to determine
their effects on weathering rates in the root zone, is lacking. This makes it difficult to estimate the impacts of early lycophytes



on the climate of the past. Moreover, since many of the Palaeozoic lycophyte species, notably the tree lycophytes are now
105 extinct, it is not straightforward to infer their geochemical impacts directly from recent extant lycophytes. Also, fossil records
and proxy studies, which provide key information on morphological properties of early lycophytes and their approximate
geographical distribution, are usually not sufficient to derive the extent of biogeochemical impacts of early vegetation in a
quantitative way. It is thus necessary to develop an approach that can estimate vegetation properties for the Silurian, based on
available information, such as climate reconstructions and known physiological mechanisms.

110 Here, we introduce a process-based model, called LYCOM, which simulates lycophyte properties and is able to simulate
diverse extinct plant communities based on given climatic conditions. This is complemented by a simple limit-based weathering
model (Arens and Kleidon, 2011) which is utilized to determine the biotic enhancement of weathering by lycophytes. We test
if the model can predict realistic lycophyte properties for a range of prescribed current climatic conditions, and assess whether
the organisms have a significant impact on weathering rates. The current study focuses on the impacts of roots and stomata of
115 lycophytes on hydrological processes as well as weathering of rocks, as the first step to a more quantitative understanding of
the impacts of early vascular vegetation on global biogeochemical cycles and climate of the past.

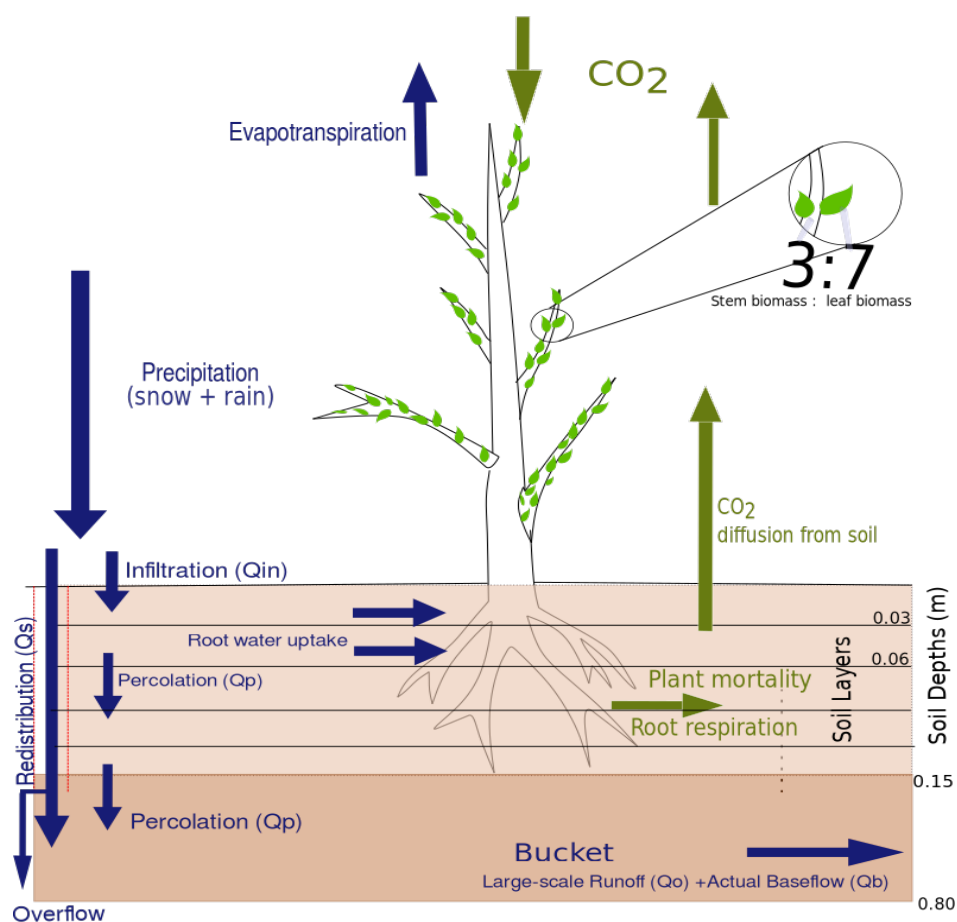
2 Methods

2.1 Lycophyte Model (LYCOM)

The process-based vegetation model used in the current study aims at a general representation of lycophytes for estimating
120 the productivity and physiological properties of these organisms under a broad climatic range. LYCOM follows other dynamic
global vegetation models (DGVMs) closely regarding the representation of plant properties and functioning (Randerson et al.,
2009). Vegetation is represented as a set of carbon pools, namely below and above ground, corresponding to the roots and
shoots with leaves. The balance of these pools depends on Net Primary Productivity (NPP), which is simulated as a function of
climate forcing. The current version of LYCOM differs from other vegetation models in some aspects. Stomatal conductance,
125 for instance, is described as a function of soil water content and potential evaporation, instead of using the Vapor Pressure
Deficit (VPD) as the controlling factor for the calculation of photosynthesis (Sellers et al., 1996; Lawson et al., 2010). The
main reason for this choice is that VPD does not capture the possibility of water stress of plants due to transpiration of water
into saturated air (at low VPD), which is driven by the energy balance, and also water stress due to low soil moisture. Since
we ultimately want to apply LYCOM to the Silurian period, we prefer a general approach that considers all relevant factors
130 affecting stomatal conductance over a specific parameterization, which may be more accurate for the present day, but might
not hold for the geological past. Another difference between LYCOM and other DGVMs is the representation of leaves and
stems. To account for the particular morphology of lycophytes, the above-ground biomass is distributed in the form of inclined
cylinders, representing the stems, with small-sized leaves attached to the sides (see Fig. 2) instead of a detailed and complicated
branching structure occurring in most plants. The vertical distribution of roots simulated in LYCOM is similar to other DGVMs
135 with an exponential decrease in biomass distribution with depth.



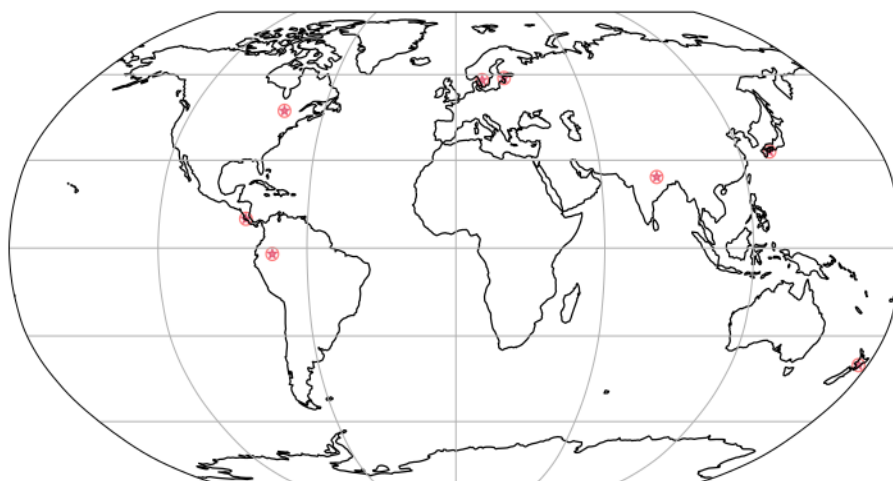
Figure 2. The rootprofile and general soil scheme comprising of the 5 layered top soil upto 15 cm followed by a bucket extending upto 0.80 meters is represented along with the hydrological profile and carbon pathways



In contrast to most global vegetation models, which use plant functional types, LYCOM explicitly represents physiological variation concerning several key characteristics of plants. This means that the ranges of observed physiological parameters derived from literature are sampled by a Monte-Carlo algorithm to generate hypothetical “species” which will be referred to as strategies in the article. These do not correspond directly to any particular lycophytes in the real world but represent the diversity of physiological strategies for lycophytes instead.



Figure 3. The locations used for the simulations are found in the following regions: United States of America (USA)[47° N 78° W], Costa Rica (CR) [10° N 85° W], Sweden (Swe) [58° N 13° E], Estonia (Est) [58.75° N 24° E], Japan (Jap) [33° N 133° E], New Zealand (NZ)[40° S 176° E], Peru [2° S 74° W]



In this way, the response of a plant community of unknown composition with regard to a large range of environmental conditions can be simulated, and the effects of the adapted community on biogeochemical processes can be estimated. This modeling approach is more flexible compared to simulating a low number of “average” functional types with fixed properties, and it has already been successfully implemented in the JeDi-DGVM (Pavlick et al., 2013), and was further developed in the LiBry-DGVM for lichens and bryophytes (Porada et al., 2013). LYCOM is based in parts on the LiBry model. Another advantage of simulating diversity explicitly is the possibility to represent extinct species in the model for which direct current analogs are lacking. The LiBry model, for instance, has already been applied to simulate biogeochemical effects of early non-vascular vegetation in the Ordovician period (Porada et al., 2016).



Variation in the physiological features of different lycophyte strategies in LYCOM results in differences regarding their
150 carbon balance. To acquire new carbon, lycophytes have to invest their carbon resources into structures for carbon uptake.
Since carbon can be allocated to different parts of the plant (leaves, roots) this represents a trade-off. The various strategies
simulated by the model differ in their carbon allocation and are thus adapted to different climatic conditions. Hence, through
analyzing the relative performance of each strategy, we can identify the key ecophysiological properties which determine the
distribution of lycophytes under any given recent or past climate.

155 2.2 Model Description

To determine both the spatial distribution of lycophytes as well as their impacts on weathering rates, it is necessary to quantify
the carbon balance of the organisms and its dependence on climatic conditions. LYCOM includes three carbon pools for
lycophytes: below-ground (root) biomass and above-ground biomass, which is subdivided into a pool for leaves and another
for stems. Gains in biomass result from Net primary production (NPP), while losses are due to mortality, which includes
160 both above-ground litterfall and root turnover. NPP is calculated as the difference between photosynthesis and respiration
(partitioned into leaf and root respiration), which are computed in LYCOM as functions of environmental climatic conditions,
such as available water, light, and temperature. Thereby, root water uptake and subsequent transpiration through leaves connect
the carbon to the water balance in the model. In the following sections, we describe the various equations aimed to describe
biochemical and physical processes in LYCOM.

165 2.2.1 Soil scheme and hydrology

To simulate the water balance at the land surface and its connection to vegetation processes, we developed a hybrid soil scheme,
consisting of a root zone, which is subdivided into 5 layers, and a “bucket” below the root zone. The layers have a thickness
of 3 cm each and the bucket has a depth of 65 cm, resulting in a total depth of 0.8 m. This scheme aims to take into account
the effects of the vertical distribution of soil water on the success of simulated strategies of lycophytes that differ in their root
170 profiles. Since extant lycophytes, however, can only reach a maximum rooting depth of approximately 15 cm (Matsunaga and
Tomescu, 2016), we resolve the soil water profile and its effects on the root profile up to this depth (Fig. 2). The inclusion of
a bucket as water storage below the layers is necessary to simulate a realistic overall partitioning of rainfall at the land surface
into evapotranspiration and runoff, i.e. avoid overestimation of runoff due to frequent saturation of the soil.

Rainfall serves as the primary water source for the soil and enters the first layer of the root zone. From there, water percolates
175 down into the next layer, as a function of the relative water content of the respective layer, limited to the actual amount of water
contained in the layer (equation 1-3). This sequence is repeated until the bucket is reached. In each layer, surplus water, which
results from the exceeded water storage capacity of a layer, directly enters the bucket. This is justified by the spatial resolution of
the model, which is designed to ultimately run at the regional or global scale. If the surface soil is saturated locally, overflowing
water usually infiltrates into the surrounding soil, and does not immediately contribute to surface runoff. Only in case, the soil



180 is saturated at a large scale, which corresponds to the bucket being near saturation, surface runoff is generated in the model,
which then contributes to total runoff.

$$Q_{in} = Rainfall + snowmelt(.layer1) \quad (1)$$

$$W_u = W_O + (Q_{in} - Q_p) \cdot p_{dt} \quad (2)$$

185

$$Q_p = \min(Q_{p0} \cdot S, W_u/p_{dt}) \quad (3)$$

where, Q_{in} = Incoming water into layers (rain + snow melt - Interception by surrounding vegetation (for first layer)), p_{dt}
= timestep, Q_p =percolation(which becomes the Q_{in} for the following layer) , Q_{p0} = (0.5e-7 [m/s]) Percolation under water
saturated condition, S = relative water saturation level of the layer, W_u = updated layer Water content, W_O = Initial layer water

190 content

In addition to infiltration and percolation, root water uptake changes the water content of the layered soil in the model.
Uptake of water by roots is calculated for each layer as a function of potential evapotranspiration (Monteith, 1981), which is
then modified depending on the share of the root biomass contained in the respective layer on the total root biomass (equation
4). Additionally, root uptake is limited to the available water in each layer.

$$195 \quad Q_R = \min(Q_{Rpot} \cdot Br / \text{sum}(Br), W_u/p_{dt}) \quad (4)$$

where, Q_R = root uptake from Layer, Q_{Rpot} = Potential Evapotranspiration [m/s], Br = layer biomass content, $\text{sum}(Br)$ =
Total root biomass, W_u = Water content of layer

$$Q_b = \min(Q_{b0} \cdot S_2, W_x/p_{dt}) \quad (5)$$

200 where, Q_b = Base flow, Q_{b0} = Base runoff rate [m/s], S_2 = average saturation of the bucket soil part, W_x = Water content of
bucket

The water balance of the bucket is then calculated according to the following equation:

$$W_x = W_{Ix} + (Q_p + Q_s - Q_b - Q_o) \cdot p_{dt} \quad (6)$$

205 where, W_x = Updated bucket water content, W_{Ix} = Initial bucket water content, Q_p = Percolation from the upper layers, Q_s =
Overflow from top layer, Q_b =Actual base flow , Q_o = Large scale runoff comprising of the excess water from the saturated
bucket



2.2.2 Stomatal Conductance

In LYCOM, stomatal conductance depends on two main factors: Firstly, it is controlled by the evapotranspiration ratio (ETratio), which means the ratio of the potential evapotranspiration at a given time of the day and the average potential evapotranspiration for the overall timeframe (eq. 8). Through the ETratio (eq. 7), a normalized estimate of the atmospheric water demand (and, thus, potential water stress) is defined, which is independent of empirical parameters and considers both the vapor pressure deficit and net radiation as drivers of evaporation. The motivation for this approach is the potential dependence of empirical parameterizations on recent climatic conditions and also on physiological properties of the current vegetation community, which is likely adapted to the climate. Consequently, when applied to the geological past, these parameterizations may not be valid anymore. Our approach is flexible enough to be applied to palaeo-climatic scenarios. It thereby depends on the assumption that the plant community is adapted to the prevailing average conditions, and thus using our normalized measure for atmospheric water demand will lead to a realistic response of stomatal conductance to short-term variations in the climate forcing.

The average atmospheric evaporation demand for the full-time span of the run is determined in the pre-processing. The run-time atmospheric demand is then evaluated using the following equation 7.

$$ETratio = ETdata / ETdavg \quad (7)$$

ETratio=Relative atmospheric demand to the whole run-time, ETdata= run-time atmospheric water demand, ETdavg=average atmospheric water demand for the whole runtime

The stomatal conductance is then computed as:

$$gsleaf = gs0, \text{ when, } ETratio \leq 1, \\ \text{ else, } gsleaf = (gs0) / (ETratio)^{\log p_{gs1} / \log ETrmax} \quad (8)$$

where, $gs0$ = maximum stomatal conductance, $ETratio$ = (Potential evapotranspiration at the given timestep/ Average evapotranspiration), p_{gs1} = shape parameter, $ETrmax$ = Maximum ETratio for the entire simulation, $gsleaf$ = stomatal conductance due to atmospheric demand

Secondly, stomatal conductance is limited by maximum conductance (dependent on species) and soil water availability in our model. To this end, the conductivity for water flow at the soil root interface is computed, which is proportional to the soil water content (eq. 10). The realized stomatal conductance is then limited to root conductance. In this way, also the impacts of soil water stress on stomatal conductance can be taken into account, in addition to the atmospheric drivers.

$$gsroot = gs0 \cdot S1 \quad (9)$$

$$gsfinal = \min(gsleaf, gsroot) \quad (10)$$

where, $gsroot$ = stomatal conductance determined by average layer water content, $gsfinal$ = stomatal conductance limited both by soil water availability and atmospheric demand, $S1$ = average saturation of the layered soil part.



2.2.3 Above and below ground biomass

In LYCOM, plant growth corresponds to Net Primary Production (NPP), which is based on the simulated net photosynthesis averaged over one month. Thereby, net photosynthesis is computed as gross photosynthesis minus respiration according to Farquhar and Von Caemmerer (1982).

$$f_{GPP,CO_2} = v_{cm} \cdot \frac{(CO_2 - P)}{CO_2 + K_c \cdot \frac{1.0 + O_2}{K_o}} \quad (12)$$

where, $f_{GPP,L}$ = Light limited gross primary production, f_{GPP,CO_2} = Carbon dioxide limited gross primary production, v_{cm} = maximum specific carboxylation rate, J = actual rate of electron transport, CO_2 = CO_2 concentration, O_2 = Oxygen concentration, P = CO_2 compensation point, K_c, K_o = Michaelis-Menten constants of carboxylation and oxygenation reactions

Gross photosynthesis is simulated as the minimum of a light-limited and a CO_2 -limited rate. The light-limited rate is an increasing function of the absorption of light and is constrained by the maximum rate of the electron flux (J_{max}). The CO_2 -limited rate is an increasing function of the CO_2 concentration in the chloroplasts and saturates at high values of CO_2 concentration, the maximum rate being VC_{max} . The detailed formulation can be found in Porada et al. (2013).

$$GPP = \min(f_{GPP,L}, f_{GPP,CO_2}) \quad (13)$$

where, GPP = Gross primary production

Photosynthesis peaks around an optimum surface temperature estimated for the individual strategies (June et al., 2004), and the estimation of respiration is done using a common empirical temperature response framework with respect to Q_{10} (eq. 15) (Vanderwel et al., 2015). The Gross and Net Primary Production (GPP and NPP) are calculated:

$$NPP = GPP - R \quad (14)$$

$$R = R_0 \cdot Q_{10}^{((T - T_{opt})/10.0)} \quad (15)$$

where, NPP = Net primary production, R = Respiration, R_0 = Reference respiration rate at $10^\circ C$, Q_{10} = Q_{10} value of respiration, T = Temperature on the surface of the plant, T_{opt} = Optimum temperature

The pore space CO_2 concentration inside the leaves is a function of the stomatal conductance which is in turn controlled by the water availability in soil (eq. 10). Thereafter, we have considered a steady-state assumption of pore space CO_2 between diffusion and the net photosynthesis which is in turn dependent on the respiration. This drives the light and CO_2 limited Farquhar and Von Caemmerer (1982) assimilation model of photosynthesis. The rest of the scheme is analogous to the LiBry model (Porada et al., 2013).



Plant growth is often limited by water availability, which causes the organisms to invest carbon from NPP into root structures to increase access to soil water. Since plant growth is also limited by light, carbon needs to be invested into stems and leaves, too. This leads to a trade-off regarding the allocation of the assimilated carbon to either above- or below-ground biomass. To address this key physiological trade-off, LYCOM includes a flexible allocation scheme that is adaptive to the prevailing atmospheric conditions, i.e. whether the plant photosynthesizes under light-limited or CO₂-limited (i.e. water-limited) conditions. The light-limited photosynthesis enhances allocation of NPP into shoot and leaves while the CO₂ limitation leads to the accumulation of root biomass (equation 16,17 and 18). The distribution and amount of root biomass and also above-ground biomass is key to the quantitative estimation of impacts of vegetation on multiple biogeochemical processes, such as microbial respiration of soil organic matter which is linked closely to chemical weathering.

Equation 16 and 17 determine the amount of assimilated carbon (NPP) assigned to root biomass with depth depending on the relative amount of limiting factors for photosynthesis. The available root biomass B_{root} is then distributed layer-wise (B_{root_i} in equation 18), with decreasing fractions at increasing depth, which is determined by the $fracR_0$ factor (Fan et al., 2016). This ensures a decreasing cumulative root distribution profile with depth.

$$B_{root_{in}} = NPP \cdot (1.0 - fracL) \cdot (layer1) \quad (16)$$

$$B_{root_{in}} = (1.0 - fracR_0) \cdot B_{root} \cdot (layersbelow) \quad (17)$$

where NPP = Net primary productivity, $fracL$ = fraction of time where light limitation dominates during photosynthesis. In this case we allocate more biomass into leaves in order to capture more light for photosynthesis, $fracR_0$ = shape constant [0.25] for an exponential decrease of root biomass allocation with depth, B_{root} = available root biomass which is still available for allocation in this layer

$$B_{root_i} = IB_{root_i} + fracR_0 \cdot B_{root_{in}} - Mortality_i \quad (18)$$

where, B_{root_i} = root biomass of the layer i , IB_{root_i} = initial root biomass of the i^{th} layer, $B_{root_{in}}$ = Rootbiomassavailable, $Mortality_i$ = a term based on baseline mortality and the biomass allocation in soil layers

The assigning of root biomass to litterfall (equation 19) is an important aspect to focus on as it determines the silicate weathering in the soil. When the soil layer reaches its maximum root biomass holding capacity, the excess is directly assigned to litterfall (Eqn. 19). This adds to the mortality calculated in equation 18 which is in turn utilized to determine the soil carbon pool and later the weathering regime.



LYCOM considers the root respiration as well, which potentially could further affect the soil CO₂ content (equation 20). Root respiration (equation 20) is basically comprised of root maintenance respiration, which is used for keeping roots alive, root growth respiration for growing new roots as well as new root tissues, along with microbial respiration.

$$295 \quad R_{toM} = \max(0.0, B_{root_i} - Br_{max_i}) \quad (19)$$

R_{toM} = Root to direct litterfall, *B_{root_i}* = root biomass of layer, *Br_{max_i}* = Maximum layer root biomass.

$$R_{resp} = R_0 \cdot Q_{10}^{((T-T_{opt})/10.0)} \cdot (B_{root_i} / \text{sum}(B_{root})) \quad (20)$$

R_{resp} = Root respiration, *R₀* = Respiration determined by strategy-specific parameters, *Q₁₀* = Q10 value, *T* = Soil temperature, *T_{opt}* = Optimum temperature, *B_{root_i}* = Root biomass of layer, *sum(B_{root})* = Total root biomass

300 Besides roots, the hypothetical plants in the model also consist of a shoot and leaf partitioned in three to seven ratio of the total available above-ground biomass which is represented as a cylinder to emulate the vertical structure of the given plant strategies along with Leaf Area Index (LAI). The leaf to shoot ratio is analogous to the horizontal to vertical biomass ratio value derived from Zier et al. (2015). Lycophytes exhibit true roots, stems, and also scale-like leaves called microphylls which cover the above-ground part of the plant. In contrast to trees or shrubs, the scale-like nature of leaves is hard to distinguish from
305 the stem in the model and hence we assume that photosynthesizing parts of the plant in the model approximately comprise 70 % of the above-ground biomass.

This is a distinct feature of the model which departs from the traditional simple LAI approach while representing the above-ground share of biomass.

The leaf biomass (Eqn. 21) is used thereafter to estimate the LAI which is computed using equation 22.

$$310 \quad Bl = Bli + NPP \cdot \text{fracL} - \text{Mortality}_{shoot} \quad (21)$$

where *Bl* = leaf biomass, *Bli* = initial leaf biomass, *Mortality_{shoot}* = a term based on baseline mortality and the biomass production and allocation into above ground biomass

$$LAI = (\text{TotalLeafArea} / \text{GrA}) \quad (22)$$

315 *Total Leaf Area* = *Aleaf* · (*Bl* / *Drw*), *Aleaf* = Leaf area using measurement from Valdespino (2015a) and *Drw* = Dry leaf weight as measured in Leopold et al. (1981), *GrA* = Ground area (below)

The projection of the ground area covered by plants used for the calculation of the LAI used in the model assumes a random value ranging between 30 to 50 square centimeters. The range is close to the reconstruction of *Zosterophyllum shengfengense* (Hao et al., 2010) but we assume a maximum coverage of a lateral area equivalent of a square of 70 mm edge.



2.2.4 Weathering and soil carbon dioxide

320 To estimate chemical weathering rates and their biotic enhancement, we apply a simple limit-based approach Arens and Kleidon
(2011), which has already been used in other studies to quantify large-scale weathering, both for the current climate and also for
the geological past (Porada et al., 2016). This approach assumes that chemical weathering can be derived from the minimum
of a supply-limited rate, which corresponds to the provision of primary minerals into the dynamic soil profile via uplift, and
a transport-limited rate, which describes the removal of dissolved weathering products from the soil via runoff, named the
325 eco-hydrological limit. Without runoff, the soil solution would remain in a state of chemical saturation, and the weathering
reactions would stop. Consequently, the chemical weathering rate cannot exceed the rate of weathering products exported via
runoff. Furthermore, the rate of chemical weathering cannot exceed the rate of exposure of unweathered rock material at the
surface, which is equal in the steady-state to the erosion rate (see table 4).

While the supply limit is not affected by biotic processes, unless the impact of vegetation on erosion and uplift are considered,
330 the transport limit may be altered through the effect of CO_2 in the soil solution on the equilibrium concentration of weathering
products, and also through the effects of vegetation on runoff. The erosion is simply a function of the elevation of the sites (see
table 2) which is derived from the database of the National Center for Atmospheric Research called "TerrainBase" (TBASE).

Plants affect soil CO_2 mainly via two processes: Firstly, they directly release CO_2 into the soil as a result of root respiration,
and, secondly, they enhance microbial respiration due to decomposition of plant biomass originating from root turnover and
335 litter input into the soil. In LYCOM, we assume a steady-state between the incoming soil CO_2 via mortality (equation 16 -
18) and root respiration (equation 19), and the outgassing of the CO_2 from the soil. The overall carbon going into the soil
as litter is subject to diffusion and this is the primary carbon pool responsible for facilitating the weathering. Subsequently,
the concentration of CO_2 in the soil can be determined from the known atmospheric CO_2 -concentration and a soil diffusivity
equation (Jabro et al., 2012) as shown in Eqn. 23.

$$340 \text{Soil}_C = (B_r) \cdot S_d / (D_c) \cdot p_a + (\text{CO}_{2p}) \cdot S_d / (D_c) \cdot p_a + \text{CO}_2 \quad (23)$$

where, B_r = root turnover and litter input to the soil, $D_c = T \cdot \epsilon \cdot D_0 \cdot h_{mon}$, $T = 0.66$ (tortuosity constant), $D_0 = 0.05$, ϵ is
the air-filled soil porosity, h_{mon} = hours in month, CO_{2p} = Soil Carbon dioxide concentration from previous timestep, $p_a =$
22.71108/44 (Conversion constant from mass to ppm), CO_2 = atmospheric CO_2 content, S_d = Max root depth

2.3 Physiological strategies

345 The variation of physiological properties in the model is summarised in table 1. Some photosynthetic parameters such as the
stomatal conductance responsible for the diffusion of atmospheric CO_2 into the leaves is limited as shown in the aforementioned
table. The upper limit of the optimal temperature is limited between 0 and 50° C along with a restricted Q_{10} value between 1.5
- 2.3. The Rubisco kinetic limits are adjusted from Galmes et al. (2014). This is done keeping in mind that the current model
serves as a basis for paleoclimate (Ordovician) simulations when the lycophytes appeared and the mean surface temperature



350 was comparatively higher than today (Cocks and Torsvik, 2020). Furthermore, the physical realism of the lycophytes is asserted by constraining certain parameters ranges such as the leaf area (Valdespino, 2015b) or the dry weight of leaves (Leopold et al., 1981) based on literature that includes various taxonomic details of lycophytes. The rest of the scheme is analogous to the model described in (Porada et al., 2013).

Table 1. Parameters used to define the lycophyte specific model

Parameter	Description	Range	Unit	Reference
Aleaf	Specific Leaf area	0.01-0.15	mm ²	Eq. 22
Drw	Specific dry weight of lycophyte leaf	0.1-1	mg	Eq. 22
GrA	Specific projected area of lycophytes	30-50	cm ²	Eq. 22
fracTransm	Reduction of light in leaves	0.6-0.75		
gS0	Maximum Stomatal Conductance	0.2-0.35		Eq. 8
Vcm	Molar carboxylation rate of Rubisco	0.0139-26.8	s ⁻¹	
Vom	Molar oxygenation rate of Rubisco	0.391-2.5	s ⁻¹	
R0	Reference maintenance respiration	$1 \cdot 10^{-8} - 8.5 \cdot 10^{-7}$	mol CO ₂ (kg C s) ⁻¹	Eq. 15,20
Q ₁₀	Q ₁₀ value of respiration	1.5-2.3		Eq. 15
Topt	Optimum temperature of photosynthesis	273-323	K	Eq. 15,20
EactK _c	Enzyme activation energy of K _C	$5 \cdot 10^4 - 12 \cdot 10^4$	J mol ⁻¹	
EactK _o	Enzyme activation energy of K _o	$1 \cdot 10^4 - 5 \cdot 10^4$	J mol ⁻¹	
Eactv _m	Enzyme activation energy of V _{cm}	$4 \cdot 10^4 - 11 \cdot 10^4$	J mol ⁻¹	
EactJ _m	Enzyme activation energy of J _{max}	$3 \cdot 10^4 - 8 \cdot 10^4$	J mol ⁻¹	

2.4 Weighting scheme

355 The weighting scheme used to calculate the resulting productivity depends on the allocation of root and above-ground biomass (equation 24, 25, 26). For obtaining a representative value we scale the productivity of all surviving strategies by their weights. This yields an averaged representative NPP (table 3) and soil CO₂ which would be difficult once the dominant species is solely chosen for the purpose. To eliminate overestimation, we consider the root as well as Leaf biomass for the weighing scheme. In table A1 a comparative chart of the productivity by weighted mean, mean, and that of the dominant species is summarised.

$$360 \text{ weightedNPP} = \sum (NPP_{ji} \cdot W_i) \quad (24)$$



$$NPP_j = \frac{1}{30} \sum_{n=1}^{30} (NPP_{nj}), j = 1, 2, \dots, 12 \quad (25)$$

$$W_i = \frac{(M_i/\bar{M}) + (Lai_i/\bar{Lai})}{\sum ((M_i/\bar{M}) + (Lai_i/\bar{Lai}))} \quad (26)$$

365 where, NPP_{ji} = monthly mean NPP of species i , W_i = Weight calculated for species i , NPP_j = monthly NPP averaged over 30 years, M_i = Root biomass accumulated over 30 simulation years, \bar{M} = Mean Root biomass for all surviving species, Lai_i = Leaf area Index at the last time step, \bar{Lai} = mean LAI of the surviving species at the final time step

3 Model setup and validation

The performance of LYCOM is assessed using gas exchange measurements of photosynthesis by lycophytes under varying ambient conditions, such as temperature, carbon dioxide concentration, and photosynthetic photon flux density (PPFD)) (Soni et al., 2012). The data used for the purpose is obtained for *Selaginella bropteris* (see figure 4 dashed lines). This aims to confirm the ability of LYCOM to replicate real species and affirms the realism of our approach. Moreover, certain parameters ranges, for example, the habitable temperature range (T_{opt} in table 1) of lycophytes are determined using the data derived from Soni et al. (2012).

375 3.1 Model Setup

We run LYCOM locally for seven locations (listed in table 2) with a 2.812-degree spatial resolution data for 30 years between 1958 through 1989 with an hourly time step, simulating 100 different physiological strategies one at a time and evaluate their survival rates. The meteorological forcing data set used for the purpose is derived from WATCH Forcing Data (WFD) by making use of the ERA-Interim reanalysis data (Weedon et al., 2018). Besides, the model setup is initialized with close to present atmospheric composition of CO_2 concentration of 400 ppm and an oxygen content of 210000 ppm. The soil porosity is constrained to a relative value of 0.45 with a percolation rate of $0.5 \times 10^{-7} \text{ m s}^{-1}$ between the layers and an average baseflow of $1.0 \times 10^{-8} \text{ m s}^{-1}$ from the bucket.

3.2 Model validation

The chosen study sites encompass various climate zones, to assess if the model can capture the productivity and viability of the local lycophyte communities. The chosen sites are characterized by a high occurrence of lycophytes, as determined based on the Global Biodiversity Information Facility (GBIF, www.gbif.org).

The study by Ghiggi et al. (2019) provides data that is suitable to evaluate the hydrological cycle achieved via the hybrid soil hydrological scheme in LYCOM.



Although the physiological evolution of lycophytes is well documented there is a significant lack of literature concerning
390 biochemical properties and also the characteristic productivity range of lycophytes under various climate regimes. Hence,
our validation of the model is limited. However, the on-site measurements of productivities of *Lycopodium annotinum* and
Lycopodium clavatum in Estonia by Tosens et al. (2016) in May and early June provides an order-of-magnitude estimate in
this regard, which improves our ability to evaluate LYCOM. Both *Lycopodium annotinum* and *Lycopodium clavatum* have a
widespread distribution across several continents today and are the most common species in Estonia (gbif.org). A Similar study
395 by Campany et al. (2019) in Costa Rica affirms a robust model performance.

3.3 Parameters of LYCOM

As described in the methods section, LYCOM represents the physiological diversity of lycophytes via generating multiple
strategies, which are closely analogous to thriving lycophyte species and the intra-specific diversity of lycophytes is accounted
for in the physiological processes implemented in the LYCOM model. The distinguishing features of lycophyte strategies are
400 represented by 14 parameters and their corresponding ranges. To generate the lycophyte strategies, these 14 characteristic
parameters are assigned through randomly sampling ranges of possible values (table 1). Assignment of parameter values is
performed in two steps: (a) for each strategy, a set of 14 random numbers uniformly distributed between 0 and 1 is sampled.
The random numbers are generated by a Latin Hypercube algorithm (McKay et al., 2000). (b) These random numbers are
used to map values of the parameters from permissible ranges particular to lycophytes which are derived from literature. The
405 particulars of the equations utilized in the model are briefly described in Table 1.

Table 2. Various characteristics of the sites where the model is run including the local relief, and a comparison of the runoffs from the model
and historical runoff data between 1958 and 1988

Location	Elevation (m)	Runoff, historical: (mm/yr/m ²)	Runoff, model: (mm/yr/m ²)
USA	168	446	536
CR	700	1545	2134
Swe	260	442	544
Est	175	199	282.3
Jap	523	774	823
NZ	550	536	523
Peru	250	1837	2605

4 Results

The modeled lycophytes cope well at all the sites except in India, where the plants die due to water stress. The aforementioned
run is undertaken to incorporate the microclimate of *Selaginella bryopteris* from where the sample was collected by Soni et al.



(2012). The study forms the basis of the light, CO₂, and temperature dependence of productivity, for model calibration (Figure 5). Out of 100 strategies a maximum of 46 species survive in New Zealand followed by the USA which features 41 surviving strategies. The climate of Sweden suits 24 varieties of the generated species, and that in Costa Rica the number fixates to 30. The prevailing weather conditions in Japan and Peru support 32 and 24 strategies respectively. In India, none of the strategies survive 30 simulation years as shown in Table 2, and Estonia features the least number of surviving strategies of 18.

The measured productivity of *Lycopodium clavatum* and *Lycopodium annotinum* in Estonia by Tosens et al. (2016) range around 1.4 $\mu\text{mol CO}_2 \text{ m}^{-2} \text{ s}^{-1}$ and 1.7 $\mu\text{mol CO}_2 \text{ m}^{-2} \text{ s}^{-1}$ for the respective species. The productivity range in LYCOM model varies from 0.5 $\mu\text{mol CO}_2 \text{ m}^{-2} \text{ s}^{-1}$ to 1.23 $\mu\text{mol CO}_2 \text{ m}^{-2} \text{ s}^{-1}$ in May and early June for five dominant species possessing the maximum weights (Eqn. 26). The ecophysiological study of *Selaginella*, an early lineage vascular plant group from a tropical forest understorey in Costa Rica (Campany et al., 2019) in June exhibits a range of net photosynthesis from 1.8 to 5.8 $\mu\text{mol CO}_2 \text{ m}^{-2} \text{ s}^{-1}$. The mean productivity of the top ten strategies (by weights) over the thirty-year simulation period for June varies between 1.07 and 2.42 $\mu\text{mol CO}_2 \text{ m}^{-2} \text{ s}^{-1}$ in the model. The higher productivity range in the study results from the prevailing atmospheric temperature, which ranges between 24 and 29 °C during the on-site measurement while in the model the temperature range in June varied from 13 to 25 °C between 1958 and 1988 with a mean temperature of 21 °C which is significantly lower than the aforementioned study.

In general, the LYCOM simulates high weighted productivity (see table 3) at the tropical site in Costa Rica of 245.37 gC per m² per year, followed closely by the area in New Zealand 178.35 gC per m² per year which shows a reverse seasonality compared to other locations (Figure 4) which are situated in the Northern hemisphere. The mainland around the great lakes in the USA shows annual productivity of 128 gC per m² and that in Sweden and Estonia ranging around 146.7 and 126.03 gC per m² respectively which is comparatively low as a result of the local climate that restricts the high productivity to the summer and renders a poor productivity in other times of the year. Peru with a higher average year-round temperature provides a reasonably better climate for lycophytes resulting in productivity of 170.09 gC per m² per year.

Table 3. LYCOM outputs: survival rates, Leaf Area Index, weighted Net primary production and a weighted Soil CO₂ content

Sites	Survival rate (%)	LAI	NPP (gC/m ² / Yr)	Soil CO ₂ (ppm) Yearly Average
USA	41	1.88	128.15	10104
CR	30	4.51	245.37	77330
Swe	24	1.73	146.70	10880
Est	18	0.83	126.03	8710
India	0	0.00	0.00	400.00
Jap	32	2.17	132.28	11940
NZ	46	3.91	178.35	12320
Peru	24	2.46	170.09	53640



We averaged the weighted monthly productivity over a 30-year seasonal cycle to obtain an average measure of annual plant growth (table 3). We use a weighting scheme (see methods) to generate weighted NPP to obtain a mean seasonal cycle over 30 years (Figure 4). LYCOM can capture the seasonality with the highest productivity over the summer months. The productivity is solely a function of the local climate and is clear from figure 4.

435 The assessment of the net assimilation rate is undertaken to evaluate the model performance as mentioned in the section model calibration, to verify its capability to reproduce the lycophyte-specific lab measurements with our newly imposed parameter ranges (Table 2). The model performs reasonably and increased photosynthetic productivity is observed with an increase in photosynthetic photon flux density (PPFD) and reached saturation at $600 \mu\text{mol m}^{-2} \text{s}^{-1}$ for all strategies with a steeper slope as opposed to Soni et al. (2012) where they observed a saturation around $800 \mu\text{mol m}^{-2} \text{s}^{-1}$. The temperature
440 response studies in Soni et al. (2012) showed a gradual increase until 40°C and dropped marginally beyond that, a behavior well captured in our calibration (see Fig. 3) with a slightly lower maximum (around $7 \mu\text{mol m}^{-2} \text{s}^{-1}$) in all strategies. Photosynthetic response to carbon dioxide levels is in close consistency with that of *Selaginella bryopteris* for strategy 53, while the rest of the strategies exhibit saturation at higher maxima. We use four strategies to calibrate since the generated strategies are not a direct representation of a single species of lycophyte. This gives a relatively good idea of the model behavior under
445 various conditions for unique strategies.

Runoff is generated in LYCOM when water input by rainfall or snowmelt exceeds the water-storage capacity of the soil, with consideration of water loss via plants according to the climatic demand and stomatal regulation. Hence climate and vegetation are pivotal to the calculation of the runoff of the model. Table 2 confirms the realistic nature of our hydrological approximations and we obtain values of runoff (mean yearly runoff) from LYCOM which are comparable to historical runoff data between 1958
450 and 1988 Ghiggi et al. (2019). In general, the model runoff is overestimated when compared with literature (Ghiggi et al., 2019) except for the location in New Zealand where LYCOM slightly underestimates the annual runoff per unit area (m^2). The model renders an average runoff of 2605 mm per year in Peru and 2134 mm per year for Costa Rica, followed by 823 mm in Japan (see table 2). This overestimation can be attributed to the fact that only the layered topsoil is subject to transpirational loss as opposed to the conditions in a real forest or vegetated regions since the roots of modern plants penetrate deeper soils. The
455 loss by transpiration is several folds higher than we capture in the current model which simulates only one kind of vegetation i.e. lycophytes. In addition, the soil water saturation determines the amount of CO_2 diffusing out of the soil. The water in the soil acts as an inhibitor to the diffusion of CO_2 through pathways of available pore space. The more the soil saturates, the lower are the CO_2 emissions. The concentration of soil CO_2 (see fig 4) is thus coherently linked with the rainy season and productivity (see 4). This effect can be prominently noticed at some locations, namely, in Costa Rica, when both the productive
460 season and most rainfall coincide leading to a high content of soil CO_2 in June. The effect of both productivity and rainfall on carbon content in soil can be seen in some cases as well, such as in Sweden and Estonia, where the most productive months for lycophytes are May and June but soil CO_2 peaks slightly in August in the rainy months.

The resulting soil CO_2 concentration after diffusion forms the basis of the weathering estimate in the post-processing of the model.

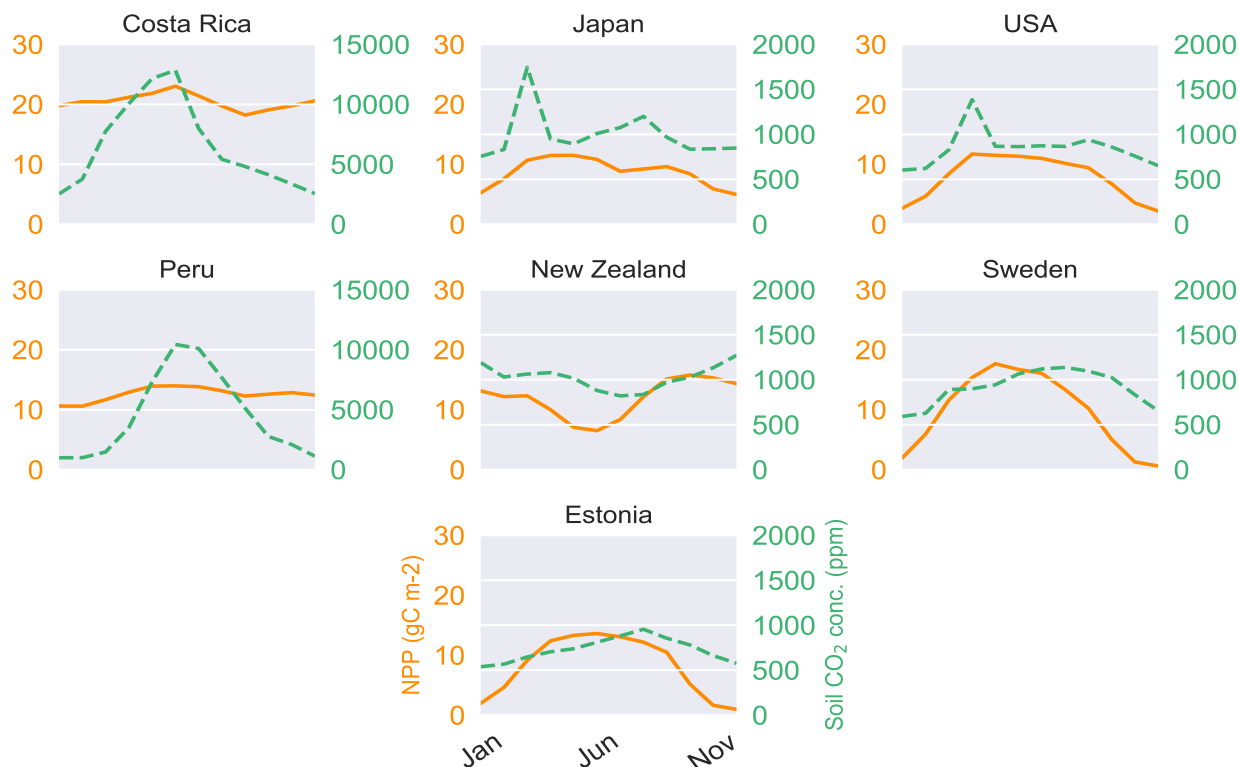


Figure 4. Annual cycle of weighted net primary productivity (solid lines) and Carbon dioxide concentration (dashed) in the soil

465 Soil CO₂ (see table 3) concentration, which is primarily a function of the productivity and soil water saturation, is seen to reach the maximum level in Costa Rica on a yearly average scale of 77330 ppm followed closely by the location in Peru where the average carbon dioxide content in soil is averaged at 53640 ppm on a yearly scale (table 3) over 30 years. Even though the seasonality of the soil CO₂ show a close relationship with productivity (Figure 4), we identify a broad range of soil CO₂ values over the study sites with the overall minimum at the study site in the USA where the NPP is low as well.

470 The supply-limited calculation of weathering rates (Arens and Kleidon, 2011) is a unique approach, where chemical weathering of silicate minerals in the soil is limited either by erosion rate or by runoff, the latter being the so-called eco-hydrological limit. Furthermore, LYCOM accounts for the effect of soil CO₂ on the maximum saturation state of the soil solution (see section 2.2.4). At the respective sites, the chemical weathering is evaluated using the soil CO₂ and runoff from LYCOM along with erosion. The eco-hydrological limits play a crucial role in determining the chemical weathering rates at all sites except for
475 Peru and Costa Rica, where the weathering is limited by erosion. Areas with shallow relief structures result in a consequently low erosion such as lowland Peru where weathering by lycophytes becomes limited by a layer of highly weathered material blocking the access to unweathered rock substrate. We represent this potential limitation of chemical weathering implicitly by calculating the erosion rate which is essentially a function of elevation of the location. Maximum ecohydrologically limited



480 weathering rate of 0.418 and 0.451 mm rock per year for every square meter is found in Costa Rica and Peru which is repre-
sentative of the high levels of productivity. The weathering in the areas is strictly restricted by erosion (see table 4). The area
of study in Japan exhibits a weathering rate of 0.086 mm rock m⁻² per year which is comparatively higher than the simulated
areas in the USA, Sweden, and New Zealand which showcase 0.045, 0.055, and 0.055 mm rock m⁻² weathering every year
respectively.

485 A regional influence of ecohydrologically limited weathering is conceived in the sensitivity runs undertaken to get an insight
into the influence of lycophytes on weathering. In addition to the runs with (a) vegetation (lycophytes), we run the model in
(b) a vegetation-free scenario. The model run with no lycophyte is undertaken to determine the large-scale runoff and the soil
CO₂ concentration is assumed to be in equilibrium with that of the atmosphere for computation of the weathering when the
location is devoid of vegetation (scenario (b) in table 5). In general, an elevated level (see table 5) of weathering is observed
at all sites with vegetation as compared to the case without vegetation. The weathering was observed to be six-folds higher in
490 Costa Rica and almost five times in Peru with vegetation. The location-specific enhancement due to vegetation is a result of
different levels of productivity and varying hydrology. The least enhancement is recorded in around the great lakes in the USA,
followed by Sweden and Japan.

Table 4. Weathering regimes post processed using Arens and Kleidon (2011) approach from LYCOM products

Location	Chemical weathering	Erosion	Weathering rates
	(mm Rock/yr), 1	(mm Rock/yr), 2	(mm Rock/yr) min(1,2)
USA	0.053	0.045	0.045
CR	0.418	0.310	0.310
Swe	0.055	0.069	0.055
Est	0.026	0.047	0.026
Jap	0.086	0.183	0.086
NZ	0.055	0.201	0.055
Peru	0.451	0.067	0.067



5 Discussion

LYCOM represents a community of lycophytes at several local sites. The respective locations provide suitable climatic conditions for the growth of lycophytes (GBIF), and the model shows relatively high survival rates there, as pointed out in table 2. The tropical climate of Costa Rica and Peru ensure continuous productivity throughout the year, while the temperate climate in the rest of the sites results in a strong seasonal pattern (see fig. 4). Increased productivity in warmer months as compared to colder months varies over latitudes as well. Indirectly, differences in climatic conditions between the locations affect productivity levels of the plants also through soil water availability. Besides, a prominent impact of soil water can be noticed in the soil CO₂ concentration. The microclimate at the site chosen for emulating the lab sample in India is likely to be substantially different from the large-scale climate derived from the global dataset. The climate of the region is markedly drier compared to the other chosen locations in the study. Therefore, the rainfall is insufficient for the sustenance of the generated lycophyte strategies. As a result, no strategies survive through the whole simulation period at the location.

The runoff in the LYCOM model is comparable to Ghiggi et al. (2019) and the lycophyte productivity in the model is comparable to Tosens et al. (2016), and Company et al. (2019) even though the generated strategies in the model are not analogous to the species utilized for observation. This establishes LYCOM as a robust process-based vegetation model with reasonable eco-hydrological representation (table 2) given the complexity of the model. Weathering is classified in LYCOM according to the dominant limiting factor, which is either the supply of parent material or the eco-hydrological conditions. In the sensitivity study, it is apparent that the influence of Lycophytes on chemical weathering rates is substantial at the local scale (table 4). It is in fact, significantly higher than their predecessors namely, early forms of lichens and bryophytes. Aghamiri and Schwartzman (2002) explores weathering by lichens and bryophytes on rock surfaces and estimates a ranges of 0.0004 to 0.01 mm rock yr⁻¹ weathering and is comparatively lower than that of lycophytes which exhibit a greater weathering potential of 0.026 to 0.418 mm rock yr⁻¹ (see table 4).

The approach of simulating strategies encompassing various physiological properties and trade-offs adds flexibility to the model, which is advantageous in representing already extinct or evolving species. In figure 5 four species generated in LYCOM are plotted under varying ambient conditions, against assimilation rates measured in the laboratory by Soni et al. (2012). This figure depicts the potential (test species in figure (dashed lines)) of the model to closely replicate real-world species which can be achieved with an appropriate selection of parameters within the defined ranges of LYCOM.

LYCOM emulates well the behavior of the organisms under local climate at the local scale. The chosen locations as suggested being suitable to such plant communities, however, do not allow for a direct extrapolation of the effects of lycophytes at the global scale. For further assessment of biogeochemical impacts of lycophytes, it is necessary to extend the model to a large scale. Even though we cannot account for all biochemical processes existing in nature, the model accounts for the most relevant properties of lycophytes and represents the local interactions sufficiently to a certain degree. It is crucial to ensure that our modeling approach remains consistent when we upscale it in the future. LYCOM paired with the weathering model forms a crucial component towards understanding the long-term impacts of such plants on Earth's climate, as influenced by the CO₂ content of the atmosphere. Although our model can provide subsequent insights into the impacts of such plants, the study is

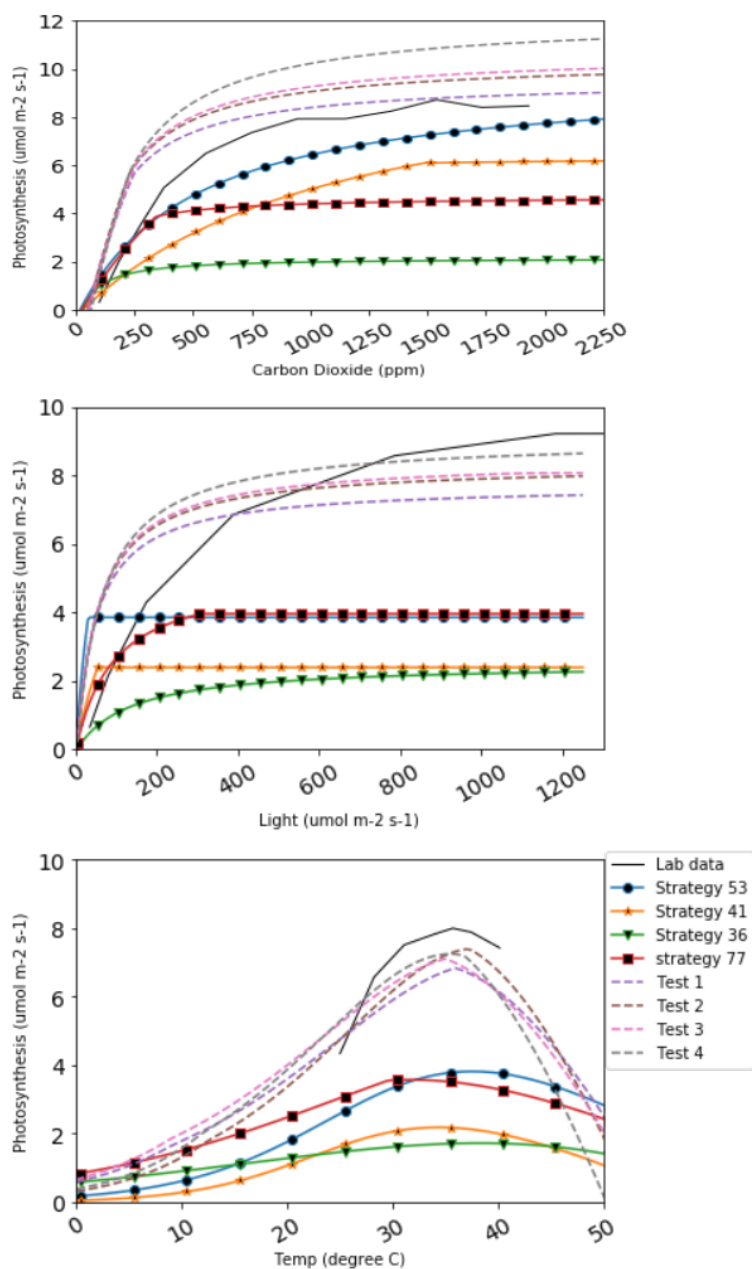


Figure 5. CO₂, light and temperature responses of 4 lycophyte strategies simulated (coloured solid lines) in LYCOM against 4 best test strategies (dashed lines) generated from LYCOM parameterization ranges in order to replicate the lab data (in black solid line (Soni et al., 2012)) as close as possible.



Table 5. comparison of supply limited eco-hydrological controlled weathering regimes (a) with and (b) without biota. In addition, the percolation rate is doubled in (a) which incorporates the impact of roots on the soil making it more porous.

Location	Chemical Weathering		Lycophyte induced weathering enhancement a/b
	With vegetation (mm Rock/yr), a	without Vegetation (mm Rock/yr), b	
USA	0.053	0.0155	3.4
CR	0.418	0.0645	6.5
Swe	0.055	0.0154	3.6
Est	0.026	0.0061	4.2
Jap	0.086	0.0233	3.7
NZ	0.055	0.0114	4.8
Peru	0.451	0.0839	5.3

restricted by a lack of data on the properties of lycophytes. Data concerning the plant physiology as well as measurements involving productivity will contribute towards a better optimization and validation of the model. Light, CO₂, and temperature curves of lycophyte species other than *Selaginella bryopteris* would not only strengthen the model performance further but help us constrain parameter ranges with better precision.

One option for improvement would be the use of high-resolution meteorological data to reduce the uncertainty of the model estimates. This would not only provide an enhanced possibility to evaluate the model performance, but also resolve the biogeochemical processes on a finer scale. Local enhancement of weathering rates could be captured better with such a setup since runoff and soil CO₂ concentration are dependent on productivity as well as hydrological balance at the respective sites. Table 6 summarises the sensitivity of weathering with increase and decrease in these components. We do not observe any disproportional enhancement factor in the weathering and thus assume that our weathering estimates are robust. Although we consider the light and water interception by the surrounding, the influence of the large forests on the water uptake from soil

Table 6. sensitivity of eco-hydrological controlled weathering regime at respective locations with (+) 20 percent enhancement and (-) 20 percent suppression of runoff and Soil CO₂ concentration, relative to the original enhancement due to vegetation from table 5

		Soil CO ₂ Concentration													
		USA		CR		Swe		Est		Jap		NZ		Peru	
		+	-	+	-	+	-	+	-	+	-	+	-	+	-
Runoff	+	1.29	1.13	1.27	1.11	1.27	1.11	1.33	1.16	1.28	1.12	1.29	1.13	1.3	1.13
	-	0.86	0.75	0.85	0.74	0.85	0.74	0.89	0.77	0.85	0.75	0.86	0.75	0.86	0.75



and humidity of the surrounding needs to be accounted for explicitly when upscaling our estimates. This may be achieved with a higher spatial resolution of the model input data representing environmental conditions.

540 6 Conclusions

The process-based lycophyte model LYCOM performs reasonably at the local scale. It is possible for lycophyte traits to survive in various climatic conditions and these can be represented well by the model. The productivity from the model shows strong agreement with the on-site measurements for the contemporary lycophytes. LYCOM, therefore, has the potential to be utilized beyond the range of current conditions. The study aims to lay the foundation for a global lycophyte model which could also
545 estimate the variability of atmospheric CO₂ levels and climate on geological time scales on coupling with a global mass balance model of carbon pools. The current study hints at a potential enhancement of the weathering by the lycophytes considerably higher than that of lichens but requires further exploration especially keeping in mind the nutrient limitation that has not been incorporated in LYCOM. Hence, lycophytes could be a crucial contributor to the enhancement of silicate weathering on a global scale, especially, during the periods in which the species dominated the flora. Further studies delving into the
550 geochemical changes as a result of the advent of lycophytes could give us detailed insights into understanding the gradual evolution of the composition of the atmosphere today.

The study is restricted by two primary factors. Firstly, the current coarse resolution of the dataset in use poses a risk of averaging the real behavior of the plant species and therefore might mask out a higher potential impact of the lycophytes on weathering rates. Secondly, poorly sampled physiological properties of lycophytes make it difficult to evaluate the model.
555 Further enhancement and extension of the lycophyte datasets are thus required, which would require a collective effort of the research community. The current work attempts to map out a relatively new field of research that has shown to hold a lot of potentials based on this preliminary work. The work aims to draw scientific interest in the field and try to incorporate these details in works such as the Paleoclimate Modelling intercomparison project (Otto-Bliesner et al., 2021).

Data availability. The input data can be accessed from Weedon, G. P., G. Balsamo, N. Bellouin, S. Gomes, M. J. Best, and P. Viterbo. 2018.
560 The WFDEI Meteorological Forcing Data. Research Data Archive at the National Center for Atmospheric Research, Computational and Information Systems Laboratory. <https://doi.org/10.5065/486N-8109>.

Author contributions. Suman Halder and Philipp Porada designed the model and Suman Halder carried out model simulations. Suman Halder prepared the manuscript with contributions from all co-authors.

Competing interests. No competing interests are present



565 *Acknowledgements.* This work has been financially supported by the Deutsche Forschungsgemeinschaft (German Research Foundation).
University of Hamburg provided computational resources.



References

- Aghamiri, R. R. and Schwartzman, D. W.: Weathering rates of bedrock by lichens: a mini watershed study, *Chemical Geology*, 188, 249–259, 2002.
- 570 Andrews, J. A. and Schlesinger, W. H.: Soil CO₂ dynamics, acidification, and chemical weathering in a temperate forest with experimental CO₂ enrichment, *Global Biogeochemical Cycles*, 15, 149–162, 2001.
- Arens, S. and Kleidon, A.: Eco-hydrological versus supply-limited weathering regimes and the potential for biotic enhancement of weathering at the global scale, *Applied Geochemistry*, 26, S274–S278, 2011.
- Bateman, R. M., Crane, P. R., DiMichele, W. A., Kenrick, P. R., Rowe, N. P., Speck, T., and Stein, W. E.: Early evolution of land plants: 575 phylogeny, physiology, and ecology of the primary terrestrial radiation, *Annual Review of Ecology and Systematics*, 29, 263–292, 1998.
- Bergman, N. M., Lenton, T. M., and Watson, A. J.: COPSE: a new model of biogeochemical cycling over Phanerozoic time, *American Journal of Science*, 304, 397–437, 2004.
- Berner, E., Berner, R., and Moulton, K.: Plants and mineral weathering: present and past, *Treatise on geochemistry*, 5, 605, 2003.
- Berner, R. A.: Atmospheric carbon dioxide levels over Phanerozoic time, *Science*, 249, 1382–1386, 1990.
- 580 Berner, R. A.: Weathering, plants, and the long-term carbon cycle, *Geochimica et Cosmochimica Acta*, 56, 3225–3231, 1992.
- Berner, R. A.: The carbon cycle and carbon dioxide over Phanerozoic time: the role of land plants, *Philosophical Transactions of the Royal Society of London. Series B: Biological Sciences*, 353, 75–82, 1998.
- Bluth, G. J. and Kump, L. R.: Lithologic and climatologic controls of river chemistry, *Geochimica et Cosmochimica Acta*, 58, 2341–2359, 1994.
- 585 Boyce, C. K. and Lee, J.-E.: An exceptional role for flowering plant physiology in the expansion of tropical rainforests and biodiversity, *Proceedings of the Royal Society B: Biological Sciences*, 277, 3437–3443, 2010.
- Boyce, C. K. and Lee, J.-E.: Plant evolution and climate over geological timescales, *Annual Review of Earth and Planetary Sciences*, 45, 61–87, 2017.
- Brodribb, T. J. and McAdam, S. A.: Passive origins of stomatal control in vascular plants, *Science*, 331, 582–585, 2011.
- 590 Campany, C. E., Martin, L., and Watkins Jr, J. E.: Convergence of ecophysiological traits drives floristic composition of early lineage vascular plants in a tropical forest floor, *Annals of Botany*, 123, 793–803, 2019.
- Cochran, M. F. and Berner, R. A.: Enhancement of silicate weathering rates by vascular land plants: quantifying the effect, *Chemical geology*, 107, 213–215, 1993.
- Cocks, L. R. M. and Torsvik, T. H.: Ordovician palaeogeography and climate change, *Gondwana Research*, 2020.
- 595 Dahl, T. W. and Arens, S. K.: The impacts of land plant evolution on Earth’s climate and oxygenation state—An interdisciplinary review, *Chemical Geology*, 547, 119 665, 2020.
- Drever, J. I.: The effect of land plants on weathering rates of silicate minerals, *Geochimica et Cosmochimica Acta*, 58, 2325–2332, 1994.
- Fan, J., McConkey, B., Wang, H., and Janzen, H.: Root distribution by depth for temperate agricultural crops, *Field Crops Research*, 189, 68–74, 2016.
- 600 Farquhar, G. D. and Von Caemmerer, S.: Modelling of photosynthetic response to environmental conditions, in: *Physiological plant ecology II*, pp. 549–587, Springer, 1982.
- Foster, G. L., Royer, D. L., and Lunt, D. J.: Future climate forcing potentially without precedent in the last 420 million years, *Nature communications*, 8, 1–8, 2017.



- 605 Galmes, J., Kapralov, M. V., Andralojc, P. J., Conesa, M. À., Keys, A. J., Parry, M. A., and Flexas, J.: Expanding knowledge of the R ubisco kinetics variability in plant species: environmental and evolutionary trends, *Plant, Cell & Environment*, 37, 1989–2001, 2014.
- Gensel, P. G. and Berry, C. M.: Early lycophyte evolution, *American Fern Journal*, 91, 74–98, 2001.
- Gensel, P. G., Kotyk, M. E., and Basinger, J. F.: Morphology of Above- and Below-Ground Structures in Early Devonian (Pragian–Emsian) Plants, *Plants invade the land: evolutionary and environmental perspectives*, p. 83, 2001.
- 610 Ghiggi, G., Humphrey, V., Seneviratne, S. I., and Gudmundsson, L.: GRUN: an observation-based global gridded runoff dataset from 1902 to 2014, *Earth System Science Data*, 11, 1655–1674, 2019.
- Gibling, M., Davies, N., Falcon-Lang, H., Bashforth, A. R., DiMichele, W. A., Rygel, M., and Ielpi, A.: Palaeozoic co-evolution of rivers and vegetation: a synthesis of current knowledge, *Proceedings of the Geologists' Association*, 125, 524–533, 2014.
- Green, J. K., Konings, A. G., Alemohammad, S. H., Berry, J., Entekhabi, D., Kolassa, J., Lee, J.-E., and Gentine, P.: Regionally strong feedbacks between the atmosphere and terrestrial biosphere, *Nature geoscience*, 10, 410–414, 2017.
- 615 Hao, S., Xue, J., Guo, D., and Wang, D.: Earliest rooting system and root: shoot ratio from a new *Zosterophyllum* plant, *New Phytologist*, 185, 217–225, 2010.
- Ibarra, D. E., Rugenstein, J. K. C., Bachan, A., Baresch, A., Lau, K. V., Thomas, D. L., Lee, J.-E., Boyce, C. K., and Chamberlain, C. P.: Modeling the consequences of land plant evolution on silicate weathering, *American Journal of Science*, 319, 1–43, 2019.
- Jabro, J. D., Sainju, U. M., Stevens, W. B., and Evans, R. G.: Estimation of CO₂ diffusion coefficient at 0–10 cm depth in undisturbed and 620 tilled soils, *Archives of Agronomy and Soil Science*, 58, 1–9, 2012.
- June, T., Evans, J. R., and Farquhar, G. D.: A simple new equation for the reversible temperature dependence of photosynthetic electron transport: a study on soybean leaf, *Functional plant biology*, 31, 275–283, 2004.
- Kelly, E. F., Chadwick, O. A., and Hilinski, T. E.: The effect of plants on mineral weathering, *Biogeochemistry*, 42, 21–53, 1998.
- Lawson, T., von Caemmerer, S., and Baroli, I.: Photosynthesis and stomatal behaviour, in: *Progress in botany* 72, pp. 265–304, Springer, 625 2010.
- Leopold, A. C., Musgrave, M. E., and Williams, K. M.: Solute leakage resulting from leaf desiccation, *Plant Physiology*, 68, 1222–1225, 1981.
- Maher, K.: The role of fluid residence time and topographic scales in determining chemical fluxes from landscapes, *Earth and Planetary Science Letters*, 312, 48–58, 2011.
- 630 Maher, K. and Chamberlain, C.: Hydrologic regulation of chemical weathering and the geologic carbon cycle, *science*, 343, 1502–1504, 2014.
- Matsunaga, K. K. and Tomescu, A. M.: Root evolution at the base of the lycophyte clade: insights from an Early Devonian lycophyte, *Annals of botany*, 117, 585–598, 2016.
- McKay, M. D., Beckman, R. J., and Conover, W. J.: A comparison of three methods for selecting values of input variables in the analysis of 635 output from a computer code, *Technometrics*, 42, 55–61, 2000.
- Montanez, I. P.: Modern soil system constraints on reconstructing deep-time atmospheric CO₂, *Geochimica et Cosmochimica Acta*, 101, 57–75, 2013.
- Monteith, J.: Evaporation and surface temperature, *Quarterly Journal of the Royal Meteorological Society*, 107, 1–27, 1981.
- Moulton, K. L., West, J., and Berner, R. A.: Solute flux and mineral mass balance approaches to the quantification of plant effects on silicate 640 weathering, *American Journal of Science*, 300, 539–570, 2000.



- Otto-Bliesner, B. L., Brady, E. C., Zhao, A., Brierley, C. M., Axford, Y., Capron, E., Govin, A., Hoffman, J. S., Isaacs, E., Kageyama, M., et al.: Large-scale features of Last Interglacial climate: results from evaluating the lig127k simulations for the Coupled Model Intercomparison Project (CMIP6)–Paleoclimate Modeling Intercomparison Project (PMIP4), *Climate of the Past*, 17, 63–94, 2021.
- Pavlick, R., Drewry, D. T., Bohn, K., Reu, B., and Kleidon, A.: The Jena Diversity-Dynamic Global Vegetation Model (JeDi-DGVM): a
645 diverse approach to representing terrestrial biogeography and biogeochemistry based on plant functional trade-offs, *Biogeosciences*, 10, 4137–4177, 2013.
- Porada, P., Weber, B., Elbert, W., Pöschl, U., and Kleidon, A.: Estimating global carbon uptake by lichens and bryophytes with a process-based model, *Biogeosciences*, 10, 6989–6989, 2013.
- Porada, P., Lenton, T., Pohl, A., Weber, B., Mander, L., Donnadieu, Y., Beer, C., Pöschl, U., and Kleidon, A.: High potential for weathering
650 and climate effects of non-vascular vegetation in the Late Ordovician, *Nature Communications*, 7, 1–13, 2016.
- Qiu, Y.-L., Li, L., Wang, B., Chen, Z., Knoop, V., Groth-Malonek, M., Dombrowska, O., Lee, J., Kent, L., Rest, J., et al.: The deepest divergences in land plants inferred from phylogenomic evidence, *Proceedings of the National Academy of Sciences*, 103, 15 511–15 516, 2006.
- Quirk, J., Leake, J. R., Johnson, D. A., Taylor, L. L., Saccone, L., and Beerling, D. J.: Constraining the role of early land plants in Palaeozoic
655 weathering and global cooling, *Proceedings of the Royal Society B: Biological Sciences*, 282, 20151 115, 2015.
- Randerson, J. T., Hoffman, F. M., Thornton, P. E., Mahowald, N. M., Lindsay, K., LEE, Y.-H., Nevison, C. D., Doney, S. C., Bonan, G., Stöckli, R., et al.: Systematic assessment of terrestrial biogeochemistry in coupled climate–carbon models, *Global Change Biology*, 15, 2462–2484, 2009.
- Raven, J. A.: Selection pressures on stomatal evolution, *New Phytologist*, 153, 371–386, 2002.
- 660 Rubinstein, C. V., Gerrienne, P., de la Puente, G. S., Astini, R. A., and Steemans, P.: Early Middle Ordovician evidence for land plants in Argentina (eastern Gondwana), *New Phytologist*, 188, 365–369, 2010.
- Sellers, P., Randall, D., Collatz, G., Berry, J., Field, C., Dazlich, D., Zhang, C., Collelo, G., and Bounoua, L.: A revised land surface parameterization (SiB2) for atmospheric GCMs. Part I: Model formulation, *Journal of climate*, 9, 676–705, 1996.
- Shukla, J. and Mintz, Y.: Influence of land-surface evapotranspiration on the earth’s climate, *Science*, 215, 1498–1501, 1982.
- 665 Soni, D. K., Ranjan, S., Singh, R., Khare, P. B., Pathre, U. V., and Shirke, P. A.: Photosynthetic characteristics and the response of stomata to environmental determinants and ABA in *Selaginella bryopteris*, a resurrection spike moss species, *Plant science*, 191, 43–52, 2012.
- Steemans, P., Le Hérisse, A., Melvin, J., Miller, M. A., Paris, F., Verniers, J., and Wellman, C. H.: Origin and radiation of the earliest vascular land plants, *Science*, 324, 353–353, 2009.
- Stein, W. E., Berry, C. M., Hernick, L. V., and Mannolini, F.: Surprisingly complex community discovered in the mid-Devonian fossil forest
670 at Gilboa, *Nature*, 483, 78–81, 2012.
- Taylor, E. L., Taylor, T. N., and Krings, M.: *Paleobotany: the biology and evolution of fossil plants*, Academic Press, 2009.
- Thomas, B. A. and Watson, J.: A rediscovered 114-foot *Lepidodendron* from Bolton, Lancashire, *Geological Journal*, 11, 15–20, 1976.
- Tosens, T., Nishida, K., Gago, J., Coopman, R. E., Cabrera, H. M., Carriquí, M., Laanisto, L., Morales, L., Nadal, M., Rojas, R., et al.: The photosynthetic capacity in 35 ferns and fern allies: mesophyll CO₂ diffusion as a key trait, *New Phytologist*, 209, 1576–1590, 2016.
- 675 Valdespino, I.: Two New Species and a New Record of *Selaginella* (Selaginellaceae) from Bolivia, *Novon*, 24, <https://doi.org/10.3417/2011022>, 2015a.
- Valdespino, I. A.: Two new species and a new record of *Selaginella* (Selaginellaceae) from Bolivia, *Novon: A Journal for Botanical Nomenclature*, 24, 96–105, 2015b.



- Vanderwel, M. C., Slot, M., Lichstein, J. W., Reich, P. B., Kattge, J., Atkin, O. K., Bloomfield, K. J., Tjoelker, M. G., and Kitajima, K.:
680 Global convergence in leaf respiration from estimates of thermal acclimation across time and space, *New Phytologist*, 207, 1026–1037,
2015.
- Vannoppen, W., De Baets, S., Keeble, J., Dong, Y., and Poesen, J.: How do root and soil characteristics affect the erosion-reducing potential
of plant species?, *Ecological Engineering*, 109, 186–195, 2017.
- Walker, J. C., Hays, P., and Kasting, J. F.: A negative feedback mechanism for the long-term stabilization of Earth’s surface temperature,
685 *Journal of Geophysical Research: Oceans*, 86, 9776–9782, 1981.
- Weedon, G. P., Balsamo, G., Bellouin, N., Gomes, S., Best, M. J., and Viterbo, P.: The WFDEI Meteorological Forcing Data, <https://doi.org/10.5065/486N-8109>, 2018.
- Wellman, C. H., Steemans, P., and Vecoli, M.: Palaeophytogeography of Ordovician–Silurian land plants, *Geological Society, London, Memoirs*, 38, 461–476, 2013.
- 690 Wickett, N. J., Mirarab, S., Nguyen, N., Warnow, T., Carpenter, E., Matasci, N., Ayyampalayam, S., Barker, M. S., Burleigh, J. G., Gitzendanner, M. A., et al.: Phylotranscriptomic analysis of the origin and early diversification of land plants, *Proceedings of the National Academy of Sciences*, 111, E4859–E4868, 2014.
- Zier, J., Belanger, B., Trahan, G., and Watkins, J. E.: Ecophysiology of four co-occurring lycophyte species: an investigation of functional convergence, *AoB Plants*, 7, 2015.



Table A1. The comparison of the Net Primary production (i) mean, which refers to the average of all surviving species (ii) weighted, according to equation 24, averaged by root and leaf biomass (iii) dominant species at the location which accumulates the maximum biomass during the simulation period

Location	NPP (Mean) gC m⁻² yr⁻¹	NPP (Weighted) gC m⁻² yr⁻¹	NPP (Dominant) gC m⁻² yr⁻¹
Costa Rica	216	245	337
New Zealand	142	178	273
Japan	104	132	195
USA	93	128	191
Sweden	115	146	192
Peru	150	170	253
Estonia	98	126	170